

First Principles Study of Polyatomic Clusters of AlN, GaN, and InN. 1. Structure, Stability, Vibrations, and Ionization

Anil K. Kandalam and Ravindra Pandey

Department of Physics, Michigan Technological University, Houghton, Michigan 49931

M. A. Blanco,^{*,†} Aurora Costales,[†] and J. M. Recio

Departamento de Química Física y Analítica, Universidad de Oviedo, 33006-Oviedo, Spain

John M. Newsam

Molecular Simulations Inc., San Diego, California 92121

Received: December 7, 1999; In Final Form: February 17, 2000

First principles calculations based on the nonlocal density approximation to the density functional theory were performed to study structures, stabilities, and vibrational properties of small (monomer, triatomic, and dimer) neutral and ionized clusters of AlN, GaN, and InN. As a general trend, triatomic isomers prefer doublet spin states, whereas triplets are predicted for the monomer and the linear dimer clusters. Both nitrogen-excess and metal-excess triatomic clusters show minimum energy configurations to be approximately linear. The most stable isomer of Al_2N_2 and Ga_2N_2 is a rhombus with a singlet spin state, though In_2N_2 is predicted not to be stable against dissociation into In_2 and N_2 . A strong dominance of the N–N bond over the metal–nitrogen and metal–metal bonds appears to control the structural skeletons and the chemistry of these clusters. This is manifested in the dissociation of neutral and singly-ionized clusters, where the loss of metal atoms is shown to be the most likely fragmentation channel, except in the case of the dimer, in which the formation of two homonuclear diatomics is favored. The vibrational modes and frequencies are also explained in terms of the different bond strengths found in the diatomic clusters.

I. Introduction

The nitrides of aluminum, gallium, and indium, and their alloys, have recently emerged as materials of choice for applications in short-wave light emitting devices and high-temperature high-power electronics.¹ This has led to numerous theoretical and experimental studies on structural, electronic, and optical properties of both surface and bulk phases and the surfaces of these materials. Research in small clusters of nitrides, however, is still lacking, though the proposed application of nitrides in microelectronic devices requires an understanding of the physical and chemical properties of the clusters at the atomic level. For example, a preparation of electronic devices generally involves the sputtering of Al in the presence of N_2 to make thin layers of AlN. However, this process can introduce surface defects which may be viewed as microclusters of AlN adsorbed over the surface of a thin film.²

In this paper, we report the initial results of a theoretical study of small nitride clusters, aiming at understanding the emergence of condensed-phase properties starting from the nanometer dimensions. Specifically, we will focus on the equilibrium properties of the monomer, triatomic species, and dimer of neutral and singly-ionized AlN, GaN, and InN. We will also analyze the ionization-induced structural transformations and the stability against various fragmentation channels.

Clusters of GaN and InN have not been the subject of any experimental or theoretical studies, to the best of our knowledge,

even in the case of GaN and InN monomers. For AlN clusters, the reported work is limited only to a few studies. These include a multireference configuration interaction (MRCI) study³ of AlN, a first principles (DFT-GGA) study⁴ of bonding in Al_nN (with $n < 6$) clusters, a density functional (LDA) study⁵ of bulklike isomers of $(\text{AlN})_n$ with $n = 1–3$ (without calculating their vibrational spectra), and calculations of AlN_3 , Al_3N , and Al_2N_2 using the second-order Moller–Plesset (MP2) perturbation theory.⁶ The work presented here therefore provides new results for Ga_nN_m , In_nN_m (with $n, m \leq 2$), and AlN_2 , along with the vibrational frequencies for Al_2N . The use of a single method for all of the clusters considered here will allow us to assess both size and chemical variation of the cluster properties. Furthermore, none of the previous studies have considered the stability against dissociation and, most importantly, ionized Al_nN_m clusters. Knowing that the mass spectroscopic studies can only yield the information on ionized clusters, the results of a theoretical study on such ionized clusters can form a basis for interpreting experimental results. It is well-known that the loss of an electron would introduce significant distortions in the corresponding neutral clusters upon ionization. The results of neutral clusters are therefore expected to be less reliable in interpreting the results of mass spectroscopic studies. It is to be noted here that the accuracy of the predictive capabilities of the present calculations will be established by a comparison of the structure and stability of isomers of AlN, Al_2N , and Al_2N_2 at various levels of theory.

The rest of the paper is organized as follows. In section II, we briefly describe the computational model used in this work.

* Corresponding author. Fax: (906) 487-2933. E-mail: mblanco@mtu.edu.

† Present address: Department of Physics, Michigan Technological University, Houghton, MI 49931.

Results and discussion of the geometrical features, vibrations, and stability will be presented for neutral and ionized clusters in section III, leaving the discussion of the chemical bonding for the second paper of the series (referred to as paper 2 hereafter (see the following paper in this issue)). In section IV, we will summarize our conclusions and provide some perspectives for future work.

II. Methodology

Calculations were performed on neutral and singly-ionized MN, M₂N, MN₂, and M₂N₂ clusters (where M = Al, Ga, and In) in the nonlocal density approximation to the density functional theory (referred to as GGA), combining the Becke exchange functional⁷ with the Perdew–Wang correlation functional.⁸ Double numeric basis sets supplemented with d polarization functions (the DNP set) were used to describe both metallic (Al, Ga, and In) and N atoms in a given cluster. This choice of basis set and exchange and correlation functional forms is based on extensive studies of Cr_nO_m,⁹ MgO,¹⁰ and GaAs clusters.^{11,12} The frozen-core approximation was also employed, which freezes the 1s², 1s²2s², 1s²2s²2p⁶, and 1s²2s²2p⁶3s²3p⁶-3d¹⁰ inner cores for N, Al, Ga, and In during the self-consistent field (SCF) calculations. The density and energy (SCF) tolerances were set to 10⁻⁶ e/bohr³ and 10⁻⁶ hartree, respectively. The cluster vibrational frequencies were computed under the harmonic approximation using analytic gradients in a two-point finite difference formula with step size of 0.1 bohr.

The geometry optimization of the linear and planar configurations of the clusters considered here was achieved by searching on a symmetry constrained multidimensional potential energy surface. Each calculation was considered to be converged when the gradient norm was less than 10⁻³ hartree/bohr and variation in total energy was less than 10⁻⁵ hartree. It is to be noted here that calculations were not performed for the low-lying spin states individually. Instead, spin unrestricted calculations in which the Aufbau principle determines the orbital occupancies were performed using the DMol program.¹³ Since the Aufbau principle generally converges toward the lowest-energy electronic configuration for a given geometry, the converged electronic state may not correspond to the lowest-energy minimum of the potential energy surface. To circumvent this possibility, we have therefore chosen several different initial geometries for the optimization of each of the structures in a given symmetry and have only reported the results corresponding to the lowest total energy minimum, if more than one were found. Analysis of the stability, fragmentation path, and normal modes was then performed only for the most stable structure for each cluster size. The first ionization potential of the various Al_nN_m, Ga_nN_m, and In_nN_m clusters was also calculated in both vertical and adiabatic approximations. In the first case, the optimal configuration of the most stable neutral cluster is kept frozen to compute the total energy of the ionized cluster. In the second case, the ionized cluster configuration is optimized to obtain the adiabatic value of the ionization potential.

III. Results and Discussion

A. Neutral Clusters: Structures. Table 1 lists spectroscopic constants for the AlN, GaN, and InN monomers. The ground state of the monomer is predicted to be a triplet in all cases, though its nature in AlN is different than that in GaN and InN. Calculations find the ground state to be ³Π ($\pi^3\sigma^1$) in AlN, while it is ³Σ ($\pi^2\sigma^2$) in both GaN and InN. In going from AlN to GaN to InN, the calculated bond length (R_e) shows an increasing trend, while the binding energy (D_e) shows a decreasing trend:

TABLE 1: Bond Lengths, Binding Energies, Vibration Frequencies, and Dipole Moments for Neutral and Ionized Monomers of AlN, GaN, and InN

	R_e (Å)	D_e (eV)	ω_e (cm ⁻¹)	μ_e (D)
AlN				
experiment ¹⁴	1.79		747	
GGA/DNP (this work)	1.82	2.74	710	3.06
GGA/6-311G** ⁴	1.80	2.78		
CASSCF ³	1.82		744	
MRCI+Q/multi- ζ ³	1.82		739	
AlN ⁺				
GGA/DNP (this work)	2.10	0.43	322	4.53
GaN				
GGA/DNP (this work)	2.06	2.45	447	2.04
GaN ⁺				
GGA/DNP (this work)	2.47	0.15	133	4.61
InN				
GGA/DNP (this work)	2.28	2.08	378	2.43
InN ⁺				
GGA/DNP (this work)	2.66	0.11	74	5.45

R_e is 1.82, 2.06, and 2.28 Å and D_e is 2.75, 2.45, and 2.08 eV for AlN, GaN, and InN, respectively (see Table 1). This is mainly due to a decrease in the strength of the chemical bond between the metallic atom and nitrogen in this series. It is also reflected in the values of the vibrational frequency (ω), which are 710, 447, and 378 cm⁻¹ for AlN, GaN, and InN, respectively.

For the AlN monomer, the calculated R_e and ω are in good agreement with the corresponding experimental data, 1.79 Å and 747 cm⁻¹, respectively.¹⁴ As shown in Table 1, our calculated results are also in very good agreement with GGA calculations with standard 6-311 G** basis sets⁴ and MRCI calculations with extended multi- ζ basis sets.³ This agreement of the calculated results with the previous calculations confirms the accuracy and reliability of the GGA level of theory along with the DNP basis sets in predicting spectroscopic constants of the nitride clusters. A previous theoretical study⁵ based on the local density approximation (LDA) reported a bond length of 1.79 Å and binding energy of 3.28 eV, showing an overestimation of the binding energy relative to the GGA value, as expected. It is to be noted here that calculations using different exchange and correlation functional forms on the AlN monomer have yielded only slightly different values with respect to those reported in Table 1.

To explain the relative stability of the various isomers of triatomic and dimeric nitride clusters, we should bear in mind the binding energies of the bonds occurring in a given configuration. For example, the computed bond dissociation energies of the N–N, Al–N, and Al–Al bonds are 9.77, 2.74, and 1.77 eV, respectively. It is therefore expected that skeletons of the stable isomers of AlN₂, Al₂N, and Al₂N₂ are governed by the relative strengths of the bond energies, favoring, in this order, the appearance of N–N, Al–N, and Al–Al sequences. Similar ordering is also expected in isomers of GaN and InN clusters. A complete list of structural parameters along with the total energies and spin multiplicities is given in Tables 2–4 for all the isomers studied in this work, whereas their structures are depicted in Figure 1.

In the nitrogen-excess triatomic AlN₂, the lowest-energy isomer has almost a linear Al–N–N configuration with C_s symmetry, closely followed by N–Al–N with C_{2v} symmetry, and the linear Al–N–N $C_{\infty v}$ isomer. The linear N–Al–N isomer ($D_{\infty h}$) is more than 5 eV higher in energy than any of these isomers. This can be explained in terms of the N–N bond. For N–Al–N, there is no such bond, while all the other AlN₂ isomers form this bond with separation close to that of the N₂ molecule. For GaN₂ and InN₂, a similar degeneracy between

TABLE 2: Spin Multiplicities, Bond Lengths (Å), Bond Angles (deg, see Figure 1 for Definitions), and Total Energies (hartree) of the Al_nN_m Polyatomic Clusters^a

	$2S + 1$	R_{Al-N}	R_{N-N}	R_{Al-Al}	α	E
AlN_2						
N-Al-N, $D_{\infty h}$	2	1.86			180	-351.751 25
Al-N-N, $C_{\infty v}^*$	2	2.15	1.16		180	-351.938 10
N-Al-N, C_{2v}	2	2.32	1.18		30	-351.939 46
Al-N-N, C_s	2	2.15	1.16		171	-351.940 46
AlN_2^+						
Al-N-N, C_s	1	3.00	1.12		168	-351.711 22
Al_2N						
Al-Al-N, $C_{\infty v}^*$	2	1.73		2.71	180	-539.502 51
Al-N-Al, $D_{\infty h}$	2	1.75			180	-539.632 53
Al-N-Al, C_{2v}	2	1.75			177	-539.632 60
Al_2N^+						
Al-N-Al, C_{2v}	1	1.73			177	-539.341 82
Al_2N_2						
N-Al-Al-N, $D_{\infty h}$	3	1.81		2.61	180	-594.197 68
N-Al-N-Al, $C_{\infty v}^*$	3	1.91, 1.72, 1.82			180	-594.307 85
Al-Al-N-N, $C_{\infty v}^*$	3	2.01	1.16	2.66	180	-594.363 44
Al-N-N-Al, $D_{\infty h}^*$	3	1.92	1.23		180	-594.382 91
Al-N-N-Al, D_{2h}	1	2.10	1.29	4.00	36	-594.388 04
$Al_2N_2^+$						
Al-N-Al-N, D_{2h}	2	2.57	1.19	5.01	27	-594.131 44

^a The superscript asterisk refers to configurations with an imaginary frequency.

TABLE 3: Spin Multiplicities, Bond Lengths (Å), Bond Angles (deg, See Figure 1 for Definitions), and Total Energies (hartree) of the Ga_nN_m Polyatomic Clusters^a

	$2S + 1$	R_{Ga-N}	R_{N-N}	R_{Ga-Ga}	α	E
GaN_2						
N-Ga-N, $D_{\infty h}$	2	1.87			180	-2034.403 27
Ga-N-N, $C_{\infty v}^*$	2	2.44	1.14		180	-2034.609 10
Ga-N-N, C_s	2	2.49	1.14		177	-2034.611 04
N-Ga-N, C_{2v}	2	2.58	1.16		26	-2034.611 33
GaN_2^+						
Ga-N-N, C_s	1	2.99	1.12		178	-2034.390 12
Ga_2N						
Ga-Ga-N, $C_{\infty v}$	2	1.84		2.83	180	-3904.846 35
Ga-N-Ga, $D_{\infty h}^*$	2	1.79			180	-3904.941 91
Ga-N-Ga, C_{2v}	2	1.79			172	-3904.941 89
Ga_2N^+						
Ga-N-Ga, C_{2v}	1	1.76			177	-3904.641 35
Ga_2N_2						
N-Ga-Ga-N, $D_{\infty h}$	3	1.81		2.50	180	-3959.521 21
N-Ga-N-Ga, $C_{\infty v}^*$	3	1.89, 1.74, 1.89			180	-3959.612 58
Ga-Ga-N-N, $C_{\infty v}^*$	3	4.47	1.12	2.81	180	-3959.706 93
Ga-N-N-Ga, $D_{\infty h}^*$	3	2.03	1.21		180	-3959.708 53
Ga-N-Ga-N, D_{2h}	1	2.20	1.27	4.21	34	-3959.714 83
$Ga_2N_2^+$						
Ga-N-Ga-N, D_{2h}	2	2.63	1.18	5.13	26	-3959.484 66

^a The superscript asterisk refers to configurations with an imaginary frequency.

the isomers of C_s , and C_{2v} , symmetry is predicted, with an energy difference of about 0.005 eV. In fact, the lowest-energy isomers of these triatomic clusters can be understood as a metallic cation bonded to a N_2 molecule either along ($C_{\infty v}$ and C_s) or perpendicular to (C_{2v}) the N-N line. The N-N separation remains nearly the same in AlN_2 , GaN_2 , and InN_2 , while the metal-nitrogen separation changes from 2.15 (AlN) to 2.49 (GaN) to 2.87 Å (InN), showing the size effect of the metallic atom in the C_s clusters.

A recent theoretical study on Al- N_2 using both MP2 and QCISD(T), with several correlation-consistent triple- ζ (cc-pCVTZ) basis sets,¹⁵ reported a minimum for the collinear approach of Al to the geometry-frozen N_2 molecule. At the minimum, the Al-N distance was in the range of 3.35–3.45 Å, with D_e about 0.05 eV. A similar calculation has been repeated here yielding the Al-N distance of 3.36 Å and D_e of 0.07 eV.

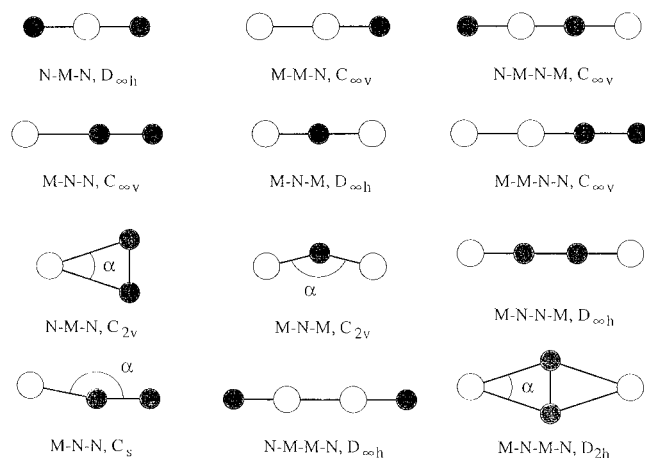
Among the linear isomers of Al_2N (Al-N-Al and Al-Al-N), the optimized configurations show that R_{Al-N} is about the same as that in the AlN monomer. However, R_{Al-Al} in Al-Al-N is 2.71 Å, as compared to 2.56 Å in Al_2 , suggesting a weaker Al-Al bond. A comparison of total energies of the two linear isomers indicates the stability of Al-N-Al over Al-Al-N by 3.5 eV. When we bend Al-N-Al facilitating the formation of an Al-Al bond, the bent isomer comes out to be nearly degenerate with the linear one, with a bond angle of 177°. Therefore, the most stable isomer of Al_2N does not seem to favor the existence of homonuclear Al-Al bonds, in agreement with the bond energies previously discussed. The computed bond length of 1.75 Å of the linear Al-N-Al isomer is in good agreement with the value of 1.74 Å obtained previously by GGA calculations employing 6-311** basis sets.⁴

The corresponding quasi-linear isomers are also predicted to be the lowest-energy structures for Ga_2N and In_2N , though the

TABLE 4: Spin Multiplicities, Bond Lengths (Å), Bond Angles (deg, See Figure 1 for Definitions), and Total Energies (hartree) of the In_mN_m Polyatomic Clusters^a

	$2S + 1$	$R_{\text{In-N}}$	$R_{\text{N-N}}$	$R_{\text{In-In}}$	α	E
InN_2						
N-In-N, $D_{\infty h}$	2	2.09			180	-5852.312 44
In-N-N, $C_{\infty v}^*$	2	2.80	1.13		180	-5852.547 74
N-In-N, C_{2v}^*	2	2.99	1.14		22	-5852.549 20
In-N-N, C_s	2	2.87	1.13		164	-5852.549 40
InN_2^+						
In-N-N, C_s	1	3.38	1.12		164	-5852.341 28
In_2N						
In-In-N, $C_{\infty v}$	2	2.09		2.92	180	-11540.702 35
In-N-In, $D_{\infty h}^*$	2	2.00			180	-11540.781 67
In-N-In, C_{2v}	2	2.01			174	-11540.781 87
In_2N^+						
In-N-In, C_{2v}	1	1.96			174	-11540.507 93
In_2N_2^b						
N-In-In-N, $D_{\infty h}$	3	2.04		2.92	180	-11595.354 50
N-In-N-In, $C_{\infty v}^*$	3	2.12, 1.96, 2.08			180	-11595.438 81
In-N-N-In, $D_{\infty h}$	3	2.29	1.20		180	-11595.571 38
In-N-In-N, D_{2h}	1	2.44	1.25	4.71	30	-11595.575 31
In-In-N-N, $C_{\infty v}^*$	3	4.66	1.12	3.18	180	-11595.584 06
In_2N_2^+						
In-N-In-N, D_{2h}^*	2	2.85	1.19	5.58	24	-11595.370 99

^a The superscript asterisk refers to configurations with an imaginary frequency. ^b It is not stable against dissociation (see Table 8).

**Figure 1.** Schematic representation of the structures of MN clusters ($M = \text{Al, Ga, In}$). The large empty circles represent metal atoms M , and the small shaded circles represent N atoms.**TABLE 5: Normal Vibrational Modes, Frequencies (cm^{-1}), and Relative Infrared Intensities (I) of Selected Configurations of the Neutral Clusters**

cluster	mode	M = Al		M = Ga		M = In	
		ω	I	ω	I	ω	I
MN_2, C_s	A'	178	0.00	88	0.00	45	0.00
	A'	219	0.00	242	0.00	229	0.00
	A'	1887	1.00	2036	1.00	2094	1.00
$\text{M}_2\text{N}, C_{2v}$	A_1	92	0.85	55	1.00	36	0.49
	A_1	498	0.00	302	0.06	202	0.03
	B_1	1014	1.00	882	0.74	783	1.00
$\text{M}_2\text{N}_2, D_{2h}$	B_{3u}	194	0.00	154	0.09	82	0.11
	B_{2u}	228	0.05	165	0.00	112	0.00
	A_g	303	0.00	174	0.01	122	0.02
	B_{1u}	505	1.00	426	1.00	368	1.00
	B_{3g}	509	0.00	456	0.00	421	0.00
	A_g	1330	0.00	1372	0.00	1421	0.00

In-N-In minimum is very shallow with respect to variations in the bond angle (see vibration frequency in Table 5). There is a small increase in the metal–nitrogen bond length, mainly due to the metal size in these triatomics. Furthermore, the linear arrangement favoring the metal–metal (Ga–Ga or In–In) bond

is found to be about 2.5 eV higher in energy relative to that containing two metal–nitrogen bonds.

For nitride dimers, both linear and ringlike configurations are considered. In the linear Al_2N_2 case, there are four possible arrangements of Al and N, namely, N-Al-Al-N , N-Al-N-Al , Al-Al-N-N , and Al-N-N-Al . Among these arrangements, the order of the bond energies of Al-Al , Al-N , and N-N is expected to be the deciding factor in determining the most favorable configuration. Our calculations do indeed show the expected order, $E_{\text{N-Al-Al-N}} > E_{\text{N-Al-N-Al}} > E_{\text{Al-Al-N-N}} > E_{\text{Al-N-N-Al}}$ (see Table 2). A similar ordering is obtained for the linear isomers of Ga_2N_2 and In_2N_2 . However, the optimized configurations of Ga-Ga-N-N and In-In-N-N seem to represent the case of a metal diatomic weakly bonded to N_2 with $R_{\text{metal-N}}$ of about 4.5 Å. This isomer favors the formation of homonuclear diatomic molecules and becomes relatively more stable with respect to the ringlike configuration in going from Al to Ga to In. Indeed, it is the lowest-energy configuration for the latter. However, as we will see later in section 3D, In_2N_2 is not found to be stable against dissociation, in contrast to Al_2N_2 and Ga_2N_2 dimers. Analysis of the normal modes of the imaginary frequencies in the In-In-N-N isomer shows that the N_2 and In_2 molecules prefer to approach in an oblique direction, yielding a lower-energy minimum of C_s symmetry that is barely stable (≈ 0.04 eV) against dissociation. Nevertheless, for the sake of consistency, we will consider the metastable D_{2h} isomer in the discussion given below. We also note here that, in all M-N-N-M clusters, $R_{\text{N-N}}$ is about 12% larger than that in the N_2 molecule, indicating the loss of triple-bond character of N_2 in these linear isomers.

In the ring (D_{2h}) configuration, the geometry optimization results in N atoms occupying the shorter diagonal of a rhombus (Figure 1). $R_{\text{N-N}}$ remains essentially the same in Al_2N_2 , Ga_2N_2 , and In_2N_2 , with the respective values of 1.29, 1.27, and 1.25 Å. On the other hand, the metal–metal separation in this series increases from 4.00 Å for Al-Al to 4.71 Å for In-In (Tables 2–4). A comparison with the nitrogen-excess triatomic (C_{2v}) cluster suggests that the resulting rhombus configuration is a consequence of accommodating an additional metal atom in the opposite side of the triatomic cluster. It would further reduce the multiple character of the N-N bond in the rhombus

configuration, thereby increasing the N–N distance ($\approx 9\%$) and decreasing the metal–nitrogen distance considerably (Tables 2–4).

In the dimer nitrides considered here, except In_2N_2 , the rhombus isomer is predicted to be the most stable isomer. A closing of the linear configuration into a rhombus yields a lowering of energy of about 0.15 eV in both Al_2N_2 and Ga_2N_2 . The calculated spin state in the rhombus configuration is a singlet, which reflects a pairing of the unpaired electrons present in the linear isomers. We note here that the GGA results on Al_2N_2 are in agreement with the MP2 and QCISD(T) calculations⁶ in predicting the stability of the rhombus over the linear Al–N–N–Al isomer. The GGA and MP2 values for bond lengths are also within 2% of each other. For example, the MP2 (GGA) values in the rhombus Al_2N_2 for $R_{\text{N–N}}$, $R_{\text{Al–N}}$, and $R_{\text{Al–Al}}$ are 1.305 (1.29), 2.062 (2.10), and 3.912 (4.00) Å, respectively.

B. Neutral Clusters: Vibrations. Analysis of the normal vibrational modes of the triatomic and dimer clusters is now performed in this section, considering only the lowest-energy isomers. For the sake of consistency, we include the C_s isomer in GaN_2 , which is almost degenerate with the C_{2v} isomer, and the metastable D_{2h} isomer of In_2N_2 . A complete list of the computed frequencies and the relative intensities is given in Table 5. It is hoped that the normal mode analysis will provide a basis for interpreting the results of future infrared (IR) experiments on these nitride clusters.

In order to assess the reliability of the computed values, we have first calculated the vibrational frequencies of Al_2 , AlN, and N_2 molecules, yielding the respective values of 330, 710, and 2283 cm^{-1} . This is in very good agreement with the corresponding experimental data¹⁴ of 350, 747, and 2358 cm^{-1} , indicating that the computed values tend to underestimate the experimental values by approximately 5%. Given the significant difference between the metal–metal, metal–nitrogen, and N–N bond frequencies, it is expected that the presence of each of these bonds will leave an unambiguous signature in the vibrational spectrum of a given nitride cluster.

The association of the computed frequencies to bond vibrations is most evident in the nitrogen-excess triatomic. The lowest frequency (see Table 5) corresponds to a bending mode, as expected. The remaining two modes correspond to stretching; the first one is associated with back and forth movement of the metal atom relative to N_2 , while the second one is the most intense IR active mode, corresponding to the N–N vibrations. The relative ordering of the frequencies is in accordance with the corresponding bond strengths in the isomer. For example, the mode at 219 cm^{-1} associated with the stretching of Al–N₂ is much smaller than that of the AlN monomer, indicating a weaker Al–N bond in AlN_2 . Likewise, the N–N bond, with $\omega_{\text{N–N}} = 1887 \text{ cm}^{-1}$, is weaker in AlN_2 than in the N_2 molecule. Interestingly, an increase of the strength of the N–N bond in the series of AlN_2 , GaN_2 , and InN_2 is reflected by the respective $\omega_{\text{N–N}}$ of 1887, 2036, and 2094 cm^{-1} .

In the metal-excess triatomic clusters, the lowest-frequency mode corresponds to the bending of the cluster while the remaining two modes correspond to symmetric (A_1) and asymmetric (B_1) stretchings of the metal–nitrogen bond. The principal contribution to the stretching modes is a coupling of the two metal–nitrogen bonds, and thus one of them is below and the other is above the frequency of the monomer, as expected. Since the most stable isomers of this series are approximately linear, we can estimate the strength of the metal–nitrogen bond in these clusters relative to that in monomers. Assuming a linear triatomic molecule with a bond force constant

TABLE 6: Difference in Charges ($\Delta Q_i = Q_i[\text{ionized}] - Q_i[\text{neutral}]$, e) of Atoms in Ionized and Neutral Clusters^a

cluster	Al	N	Ga	N	In	N
MN , $C_{\infty v}$	0.41	0.59	0.45	0.55	0.46	0.54
MN_2 , C_s	0.55	0.32, 0.12	0.76	0.10, 0.13	0.84	0.05, 0.10
M_2N , C_{2v}	0.44	0.12	0.43	0.15	0.45	0.10
M_2N_2 , D_{2h}	0.00	0.50	0.21	0.28	0.25	0.24

^a For MN_2 , the N charges are in the order proximal, distal. This difference provides the contributions of metal and nitrogen atoms toward the ionization charge.

equal to that of the monomer, the average of the squares of the triatomic stretching frequencies will then be equal to the square of the monomer frequency. Under this assumption, the monomer frequencies are calculated to be 799, 659, and 572 cm^{-1} in Al_2N , Ga_2N , and In_2N , respectively. These values are higher than the computed values of 710, 447, and 378 cm^{-1} for the AlN, GaN, and InN monomers, respectively. The metal–nitrogen bond in a metal-excess triatomic cluster is therefore stronger than that in the monomer. This conclusion is further reinforced by the fact that the metal–nitrogen separations in the triatomic molecules are smaller than those in the monomers.

For dimers, we have chosen the atomic coordinates in such a way that the cluster lies on the yz plane with the N atoms located along the y axis and the metal atoms along the z axis. Using this convention, we then relate the out of plane bending of the cluster to the lowest-frequency B_{3u} mode. Parallel displacements of N in the $+y$ direction, with the metal atoms moving toward the $-y$ direction are found to be associated with the B_{2u} mode. The breathing A_g mode mostly involves the movement of the metal cations. Among the normal modes of the D_{2h} clusters, the more intense IR active mode is the B_{1u} one, with values of 505, 426, and 368 cm^{-1} for Al_2N_2 , Ga_2N_2 , and In_2N_2 , respectively. It is related to the orthogonal displacements of the N atoms along $+y$ and the metal atoms along $-z$. Next to B_{1u} , the B_{3g} mode shows a quasi-degeneracy only in Al_2N_2 . This is due to the fact that it corresponds to a ring torsion where the movement of the two Al–N pairs is similar to that in the B_{1u} mode. Lastly, the A_g mode is a breathing mode of the N–N bond as its high frequency suggests. This bond, however, will be the weakest in the sequence $\text{N}_2/\text{MN}_2/\text{M}_2\text{N}_2$, indicating a continuous decrease in the multiple character of the N–N bond with the increase in the cluster size. We note here that the calculated results on Al_2N_2 are in agreement with those of MP2 calculations.⁶ The MP2 computed frequencies (164, 227, 353, 605, 594, and 1276 cm^{-1}) are in the same ranges that those calculated in this work (Table 5), the most notable difference being a reversal of the order of the quasi-degenerate B_{1u} , and B_{3g} modes. The MP2 relative intensities are also in complete agreement with the GGA results. For the IR active modes B_{1u} and B_{2u} , the GGA calculations find the relative intensity ratio of 0.049, while the MP2 calculations find the ratio to be 0.039.

C. Ionized Clusters. We now study the ionization-induced structural distortions in the nitride clusters by considering only the most stable isomers of the corresponding neutral clusters. We will calculate both vertical and adiabatic first ionization potentials and discuss electronic changes in the ionized clusters in terms of the difference in atomic charges (ΔQ_i) presented in Table 6. In the following paper in this issue, paper 2, we provide a detailed description of the method used to calculate the charges of atoms in both neutral and ionized clusters.

According to Table 1, the loss of an electron from the neutral monomer always increases the metal–nitrogen separation, thus lowering the stretching frequency. A comparison of the charges

TABLE 7: Vertical and Adiabatic (in parentheses) Ionization Potentials (eV) for Monomers, Triatomic Species, and Dimers of AlN, GaN, and InN

cluster	M = Al	M = Ga	M = In
MN, $C_{\infty v}$	8.55 (8.30)	8.33 (8.24)	7.72 (7.64)
MN ₂ , C_s	6.68 (6.23)	6.10 (6.01)	5.69 (5.66)
M ₂ N, C_{2v}	7.92 (7.91)	8.19 (8.18)	7.45 (7.46)
M ₂ N ₂ , D_{2h}	8.04 (6.99)	7.10 (6.26)	6.10 (5.56)

of the neutral and ionized states reveals that both nitrogen and metal atoms contribute almost equally toward the loss of an electron. This is consistent with the orbital picture where the electron comes out from a bonding orbital of the monomer. The resulting ionized monomer has therefore a weaker bond than its neutral parent.

A similar scenario is expected to occur in the nitrogen-excess triatomics, where the bonding orbital is very weak. The electron coming out of the cluster was mostly located on the metal atom (Table 6); thereby its loss increases the metal–nitrogen distance by about 6%. We find, however, a slightly different situation in the metal-excess cluster, where the electron comes solely from a nonbonding orbital located over the metal atoms, leaving the nitrogen atom unaffected upon ionization. The structural changes are almost negligible, and consequently the vertical and adiabatic ionization potentials will be very much the same in Al₂N, Ga₂N, and In₂N (Table 7).

In the nitride dimers, changes induced by ionization are quite noticeable. In all of them, the structural changes involve a decrease of the N–N distance and an increase of the metal–nitrogen distance to similar extents. This is consistent with the removal of an electron from an orbital having both antibonding character for the N–N bond and bonding character for the metal–nitrogen pairs. However, as shown in Table 6, the ΔQ of the metal atom is quite different in the three clusters: for Al₂N₂, ΔQ occurs only for the N atoms, whereas in Ga₂N₂ and In₂N₂ it is equally shared among all the atoms. The frozen picture of the ionization (i.e. without relaxing the orbitals) is likely to be the loss of an electron from an orbital mainly located over nitrogens. Both geometrical and electronic rearrangements would then probably lead to changes of different sign for the charges of Al₂N₂ relative to those of Ga₂N₂ and In₂N₂.

As shown in Table 7, the structural relaxation upon ionization generally lowers the IP values. Overall, MN₂ and M₂N₂ clusters tend to ionize relatively easier (≈ 2 eV) than the corresponding M₂N and MN clusters. Additionally, their values are within the range of the atomic IP values, which are computed to be 5.98, 5.94, and 5.56 eV for Al, Ga, and In at the GGA level of theory. Furthermore, the cluster IP values are much smaller than the IP values of the N atom and the N₂ molecule, which are calculated to be 14.53 and 15.40 eV, respectively. Thus, the results further support the association of the ionized electron to the metallic atoms in the nitride clusters studied here. In the nitride series, the IP values show a small variation with the increase in the cation size that is related to the change in the respective atomic IPs. The only experimental IP value available is 5.85 eV for AlN₂,¹⁶ which compares well with our GGA value of 6.23 eV. For AlN, the (GGA) IP value of 8.30 eV is in good agreement with the previously reported value of 8.57 eV at the SOCI+Q level of theory.³

D. Stability. We now present the results on the relative stability of neutral and singly ionized clusters with respect to their fragmentation in atoms and/or clusters. We will only consider the lowest-energy configuration for each of the clusters involved, neglecting contributions from the zero-point vibration

TABLE 8: Dissociation Energies (eV) for Neutral and Ionized Polyatomic Nitride Clusters via Various Fragmentation Paths

reaction	M = Al	M = Ga	M = In
MN ₂ → M + N ₂	0.43	0.26	0.21
MN ₂ → MN + N	7.55	7.57	7.79
MN ₂ ⁺ → M ⁺ + N ₂	0.17	0.18	0.11
MN ₂ ⁺ → MN ⁺ + N	9.51	9.80	9.77
M ₂ N → M + MN	5.24	4.31	3.49
M ₂ N → M ₂ + N	6.22	5.19	3.96
M ₂ N ⁺ → M ⁺ + MN	3.30	2.06	1.59
M ₂ N ⁺ → M ₂ ⁺ + N	4.37	2.89	2.26
M ₂ N ⁺ → M + MN ⁺	5.62	4.37	3.62
M ₂ N ₂ → M ₂ + N ₂	0.76	0.20	−0.47
M ₂ N ₂ → M + MN ₂	2.09	1.52	0.98
M ₂ N ₂ → M ₂ N + N	4.31	4.78	5.33
M ₂ N ₂ → MN + MN	6.80	6.63	6.64
M ₂ N ₂ ⁺ → M ₂ ⁺ + N ₂	−0.16	−0.17	−0.28
M ₂ N ₂ ⁺ → M ⁺ + MN ₂	1.11	1.19	1.03
M ₂ N ₂ ⁺ → M + MN ₂ ⁺	1.34	1.26	1.08
M ₂ N ₂ ⁺ → M ₂ N ⁺ + N	5.23	6.69	7.23
M ₂ N ₂ ⁺ → MN + MN ⁺	8.10	8.61	8.72

energy. Table 8 is a collection of the fragmentation energies of the polyatomic nitride clusters dissociating via several possible paths. Note that the binding energy of triatomics and dimers (i.e. the energy required for the dissociation of the molecule into the constituent atoms) is found to be very large. For example, it is computed to be −10.20, −7.97, and −12.27 eV for AlN₂, Al₂N, and Al₂N₂, respectively.

It is noteworthy that most of the fragmentation reactions are *endothermic*; that is, most of these clusters are stable with respect to their fragmentation into atoms or molecules. As is readily seen, the relative dissociation energies for the various fragmentation paths can be explained by the different strengths of the N–N, metal–nitrogen, and metal–metal bonds. Therefore, products containing two bonded N atoms are obviously favored, and this explains why the nitrogen-excess triatomic clusters are relatively less stable than the metal-excess clusters, both for the neutral and charged species. We note here that the GGA bond-dissociation energy of 0.17 eV for AlN₂⁺ into Al⁺ and N₂ is in good agreement with the previously calculated value of 0.19 eV (including zero-point energy) at the GGA/6-311++G(3df,2p)//6-311G(d,p) level of theory.¹⁷

The fragmentation leading to a N₂ molecule is thus, by far, the preferred path for all the clusters containing two nitrogen atoms, regardless of its charge. In fact, all of the ionized D_{2h} dimers and the neutral In₂N₂ dimer are less stable than their homonuclear diatomic fragmentation products (Table 8). Moreover, this particular fragmentation path will take place along the low-frequency B_{3u} bending modes. The calculated results therefore predict that the D_{2h} nitride dimers will not be detected in the photoionization experiments. This is in contrast to the results of both BN¹⁸ and MgO⁹ clusters, where the heteronuclear diatomic was the most likely fragmentation product.

In M₂N clusters, the preferred fragmentation path always leads to MN monomers, and not to M₂ diatomics. The loss of a metal atom is the preferable route for the neutral triatomic clusters, while that of a metallic cation is the most favorable fragmentation channel for the ionized triatomics.

Finally, it is worthwhile to note that the energies required to dissociate the neutral clusters via the most likely fragmentation path are much smaller than their respective ionization energies. It is therefore expected that neutral clusters would prefer to dissociate rather than ionize in the photoionization experiments, unless there is a high barrier in the dissociation channel.

IV. Conclusions

In this work, we have found that small polyatomic nitride clusters have a strong tendency to form N–N multiple bonds leading to the weakening of any existent metal–nitrogen or metal–metal bonds. Whenever there is a N atom with heteronuclear bonds only, the metal–nitrogen bond proves to be a strong bond, with short bond lengths and large force constants. The strength of these heteronuclear bonds decreases in going from Al to Ga and In. The different character of the metal–nitrogen and N–N chemical bonds present in these polyatomics is also reflected in the ionization and dissociation processes. It facilitates the removal of electrons not contributing to N–N bonds, along with fragmentations leading to N₂ molecules or metallic atoms/cations as end products. The most stable isomers are predicted to be N₂ molecules weakly bonded to metal atoms for MN₂ and M₂N₂ and strongly bonded molecules for MN and M₂N. We have also simulated the vibrational spectra of these polyatomics, which are to be tested in future infrared or Raman experiments. The vibrational modes and frequencies can be explained in terms of the different bond strengths of the diatomic clusters. The calculated ionization potentials are found to be larger than the fragmentation energies of these small clusters of nitrides. The main structural feature of these clusters, namely, the strong N–N bond, is not present in the solid-state MN compounds. Thus, it is expected that an appropriate number of heteronuclear bonds would finally be preferred to the formation of N–N bonds, and then the solid-state behavior would emerge. This would be a topic of our future work on the nitride clusters.

Acknowledgment. M.A.B. is indebted to the Spanish Secretaría de Estado de Universidades, Investigación y Desar-

rollo, for a postdoctoral grant. M.A.B., A.C., and J.M.R. are also indebted to the Spanish DGICYT for Grant PB96-0559.

References and Notes

- (1) Nakamura, S. In *Proceedings of International Symposium on Blue Laser and Light Emitting Diodes*; Yoshikawa, A., Kishino, K., Klobayashi, M., Yasuda, T., Eds.; Chiba University Press: 1996; p 119.
- (2) Belyanin, A. F.; Bouilov, L. L.; Zhirnov, V. V.; Kamenev, A. I.; Kovalskij, K. A.; Spitsyn, B. V. *Diam. Relat. Mater.* **1999**, *8*, 369.
- (3) Langhoff, S. R.; Bauschlicher, C. W., Jr.; Pettersson, L. G. M. *J. Chem. Phys.* **1998**, *89*, 7354.
- (4) Nayak, S. K.; Khanna, S. N.; Jena, P. *Phys. Rev. B* **1998**, *57*, 3787.
- (5) Grimes, R. *Philos. Mag. B* **1999**, *79*, 407.
- (6) Liu, Z.; Boo, B. H. *J. Phys. Chem. A* **1999**, *103*, 1250.
- (7) Becke, A. D. *Phys. Rev. A* **1988**, *38*, 3098.
- (8) Perdew, J. P.; Wang, Y. *Phys. Rev. B* **1992**, *45*, 13244.
- (9) Veliah, S.; Xiang, K.; Pandey, R.; Recio, J. M.; Newsam, J. *J. Phys. Chem. B* **1998**, *102*, 1126.
- (10) Veliah, S.; Pandey, R.; Li, Y.; Newsam, J.; Vessal, B. *Chem. Phys. Lett.* **1995**, *235*, 53.
- (11) Lou, L.; Wang, L.; Chibante, L. P. F.; Laaksonen, R. T.; Norlander, P.; Smalley, R. E. *J. Chem. Phys.* **1991**, *94*, 8015.
- (12) Lou, L.; Norlander, P.; Smalley, R. E. *J. Chem. Phys.* **1992**, *97*, 1858.
- (13) *Dmol user guide*, version 2.3.6; Molecular Simulations, Inc.: San Diego, CA, 1995.
- (14) Huber, K. P.; Herzberg, G. *Constants of Diatomic Molecules*; Van Nostrand: New York, 1979.
- (15) Chaban, G.; Gordon, M. S. *J. Chem. Phys.* **1997**, *107*, 2160.
- (16) Brock, L. R.; Duncan, M. A. *J. Phys. Chem.* **1995**, *99*, 16571.
- (17) Stockigt, D. *Chem. Phys. Lett.* **1996**, *205*, 387.
- (18) Sutjianto, A.; Pandey, R.; Recio, J. M. *Int. J. Quantum Chem.* **1994**, *52*, 199.
- (19) Recio, J. M.; Pandey, R.; Ayuela, A.; Kunz, A. B. *J. Chem. Phys.* **1993**, *98*, 4783.